

Nernst effect in anisotropic metals

Jeffrey Clayhold

Texas Center for Superconductivity, University of Houston, Houston, Texas 77204

(Received 14 December 1995; revised manuscript received 9 May 1996)

A formulation is given for the Nernst effect of metals with nonspherical Fermi surfaces. The Nernst coefficient Q measures the correlation of the thermopower and Hall angle at different points on the Fermi surface. As an example, some data from the high- T_c superconductor $\text{YBa}_2\text{Cu}_3\text{O}_{7-\delta}$ are discussed. Further possible applications of the Nernst effect as a probe of the cuprate superconductors are suggested. [S0163-1829(96)03533-3]

The Nernst effect, which is the transverse thermopower induced by a magnetic field, is a basic electrical transport probe of conducting materials. Perhaps too often the Nernst effect is neglected as a poor cousin of its more familiar counterparts—the resistivity, Hall effect, and thermopower. Aside from the experimental difficulty involved in the measurement, the Nernst effect is often overlooked because the standard formulation of the Nernst effect of a metal requires model-dependent interpretations of experimental results. The standard formulation¹ of the Nernst effect is, however, valid only for spherical Fermi surfaces, having preceded by a decade the modern methods of Fermi surface determination.

Accounting for anisotropy of the Fermi surface gives an additional contribution to the Nernst effect, which may be the dominant term in many materials. This contribution can be written in the simple form of the correlation of the thermopower and Hall angle around the Fermi surface. The nature of the Nernst coefficient as a correlation function should allow model-independent interpretations in many cases. As described below, in the high- T_c cuprate superconductors, Nernst effect studies may be useful probes of transport differences between the $(0, \pi)$ and (π, π) directions in k space.

The Nernst effect results from a balance of electric and thermal forces acting on the charge carriers. The electric current arising in the presence of an electric field \vec{E} and a thermal gradient $\vec{\nabla}T$ is

$$\vec{J}_e = \hat{\sigma} \vec{E} - \frac{\hat{L}^{12}}{T} \vec{\nabla}T, \quad (1)$$

where $\hat{\sigma}$ is the electrical conductivity and \hat{L}^{12}/T is the electrothermal conductivity. The total current is equal to zero during the experimental measurement, which means that the thermopower tensor \hat{S} , relating the electric field to the thermal gradient $\vec{E} = \hat{S} \vec{\nabla}T$, is $\hat{S} = (1/T) \hat{L}^{12} \hat{\sigma}^{-1}$. The off-diagonal element of \hat{S} describing the Nernst effect, in terms of the resistivity tensor $\hat{\rho}$, is

$$S_{xy} = \frac{1}{T} (\rho_{xx} L_{xy}^{12} - \rho_{xy} L_{xx}^{12}), \quad (2)$$

which is zero using the standard Boltzmann expressions for the conductivity tensor $\hat{\sigma}$ and \hat{L}^{12} if the relaxation time τ is independent of energy. Each of the four terms in Eq. (2) is,

in general, nonzero, but the combination cancels. For a nonzero result, it has been customary to expand the energy dependence of the relaxation time, $\tau = \tau_0 + (\epsilon - E_F) d\tau/d\epsilon$, yielding the familiar result for the Nernst effect in terms of the energy derivative of τ at the Fermi energy:¹

$$S_{xy} = H \frac{\pi^2}{3} \frac{k_B^2 T}{m^*} \left. \frac{d\tau(\epsilon)}{d\epsilon} \right|_{E_F}. \quad (3)$$

Equation (3) is the most-commonly cited equation for the Nernst effect for comparison with experimental results despite the difficulty of theoretically modeling the energy dependence of the relaxation time for real systems.

Equation (3) gives the first nonzero contribution to the Nernst effect for an isotropic, spherical Fermi surface. If, instead, an anisotropic Fermi surface is considered, then a potentially larger contribution is obtained, without appealing to higher-order terms such as asymmetries in $\tau(\epsilon)$. Adding together the currents, Eq. (1), from different portions of the Fermi surface is accomplished by rewriting Eq. (2) in terms of $\hat{\sigma}$ and \hat{L}^{12} and summing the conductivities and L^{12} 's: $\sigma_{\text{tot}} = \int d\zeta \sigma(\zeta)$ and $L_{\text{tot}}^{12} = \int d\zeta L^{12}(\zeta)$, where $d\zeta$ represents an infinitesimal patch of the Fermi surface. The integrands are converted to combinations of experimentally obtainable transport quantities using the low-field simplifications

$$\rho_{xy} = \theta_H \rho_{xx}, \quad (4)$$

$$S_{xx} = \frac{L_{xx}^{12}}{T \sigma_{xx}}, \quad (5)$$

$$L_{xy}^{12} = \theta_H L_{xx}^{12}. \quad (6)$$

Equation (4) is the definition of the Hall angle θ_H at low magnetic field, where $\tan \theta_H \approx \theta_H$. Equation (5) is the usual, low-field expression for the thermopower. Equation (6) is true to leading order in $\tau(\epsilon)$, $\tau = \tau_0$, producing the cancellation in Eq. (2).

The integrand $L_{xx}^{12}(\zeta)$ is replaced by the product of the local thermopower and the local conductivity $T S_{xx}(\zeta) \sigma_{xx}(\zeta)$. Similarly, $\int d\zeta \sigma_{xy}(\zeta)$ becomes $-\int d\zeta \theta_H(\zeta) \sigma_{xx}(\zeta)$. The resulting version of Eq. (2), averaged over the Fermi surface, is

$$S_{xy} = \frac{\int d\xi \theta_H(\xi) S_{xx}(\xi) \sigma_{xx}(\xi)}{\int d\xi \sigma_{xx}(\xi)} - \left[\frac{\int d\xi \theta_H(\xi) \sigma_{xx}(\xi)}{\int d\xi \sigma_{xx}(\xi)} \right] \times \left[\frac{\int d\xi S_{xx}(\xi) \sigma_{xx}(\xi)}{\int d\xi \sigma_{xx}(\xi)} \right], \quad (7)$$

with $\theta_H \ll 1$. The right-hand side of Eq. (7) is just the conductivity-weighted correlation of the Hall angle and the thermopower around the Fermi surface:

$$S_{xy} = \langle \theta_H S_{xx} \rangle_\sigma - \langle \theta_H \rangle_\sigma \langle S_{xx} \rangle_\sigma, \quad (8)$$

where the brackets represent an average around the Fermi surface and the subscripts indicate that the average is weighted by the electrical conductivity.

Equation (8) is reminiscent of a recently published expression for the classical, low-field magnetoresistance in terms of the conductivity-weighted variance of the Hall angle around the Fermi surface:²

$$\frac{\Delta \rho(H)}{\rho} = \langle \theta_H^2 \rangle_\sigma - \langle \theta_H \rangle_\sigma^2. \quad (9)$$

Both measurements, the Nernst effect and the magnetoresistance, give a zero result for spherical Fermi surfaces or near any single point on an anisotropic Fermi surface. The combined currents of an anisotropic Fermi surface produce non-zero results, and in the case of the Nernst effect, it is not necessary to appeal to higher-order terms such as $d\tau/d\epsilon$.

An illustrative application of Eq. (8) is a comparison with a measurement of the Nernst effect in the normal state of the high- T_c superconductor $\text{YBa}_2\text{Cu}_3\text{O}_{7-\delta}$.

Measuring the Nernst effect in the normal state of the cuprates is a delicate affair. The signal is typically only a few nanovolts per kelvin per tesla of applied field. The longitudinal thermopower, or Seebeck voltage, is roughly 1000 times larger than the Nernst signal. Unavoidable small contact misalignment means that the Nernst signal is often dominated by the unwanted Seebeck background signal. Separating the Nernst signal from the background signal requires not only nanovolt-scale resolution, but also high stability and reproducibility of the applied temperature gradient and voltage detection. Many of the detailed experimental considerations involved in measuring the small normal-state Nernst signal have been discussed previously.³

The sample was a commercially available⁴ epitaxial $\text{YBa}_2\text{Cu}_3\text{O}_{7-\delta}$ film with a resistive midpoint T_c of 88 K and a transition width of 3 K. The temperature dependences of the normal-state resistivity and thermopower are shown in Fig. 1(a). The negative curvature of the resistivity and the magnitude of the thermopower signal indicate that the sample is slightly underdoped. The temperature dependence of the Hall coefficient displayed the usual $1/T$ behavior for $\text{YBa}_2\text{Cu}_3\text{O}_7$, as shown in Fig. 1(b).

The importance of using thin-film samples for the measurement of the Nernst effect in brittle materials⁵ cannot be emphasized enough. In bulk samples, the magnetic-field-induced transverse thermal conductivity, or Righi-Leduc effect, generates a transverse component of the thermal gradient, $\nabla_y T \approx \tan \theta_H \nabla_x T$, where the x direction is the direction of the applied gradient. The Seebeck signal associated with the small, transverse temperature difference not only has the

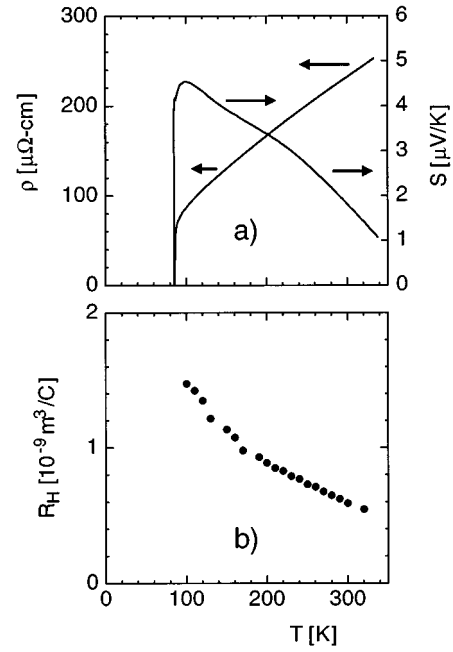


FIG. 1. (a) Temperature dependence of the normal-state resistivity, $\rho(T)$, and the thermopower, $S(T)$, of the $\text{YBa}_2\text{Cu}_3\text{O}_{7-\delta}$ sample. (b) Temperature dependence of the Hall coefficient, $R_H(T)$.

same order of magnitude as the Nernst signal to be studied, but also shares the same dependence on the magnetic field. The use of thin-film samples guarantees the isothermal condition $\nabla_y T = 0$, because the insulating substrate is the dominant thermal mass controlling the temperature gradient.

The apparatus which was used to measure the Nernst effect in $\text{YBa}_2\text{Cu}_3\text{O}_{7-\delta}$ has been described previously.³ For the measurement of $\text{YBa}_2\text{Cu}_3\text{O}_{7-\delta}$, data were taken at 10 K intervals between T_c and $T = 330$ K. For each point, the temperature was stabilized, and then the transverse, Nernst, voltage was sampled at 37 different magnetic field values between -12 T and $+12$ T. The magnetic field was along the c axis of the material and the temperature gradient and electric field were in the a - b plane.

The magnetic-field dependence of the Nernst signal S_{xy} at $T = 250$ K is shown in Fig. 2. The base-line Seebeck background signal has been subtracted. The raw data accurately display the expected linear dependence on the magnetic field. The Nernst coefficient $Q = S_{xy}/H$ at $T = 250$ K is obtained from a linear least-squares fit to the data of Fig. 2. The full temperature dependence of the Nernst coefficient of the $\text{YBa}_2\text{Cu}_3\text{O}_7$ sample is shown in Fig. 3.

The measured Nernst coefficient Q increases with decreasing temperature below room temperature, reaching a broad maximum near $T = 210$ K. The value of Q then drops rapidly to zero at a temperature just above the T_c of the sample. At still lower temperatures, the large contribution from superconducting fluctuations⁶ begins to dominate.

A more useful way to show the Nernst data is in terms of the *dimensionless* correlation $g^{S\theta_H}$ between S_{xx} and θ_H :

$$g^{S\theta_H} = \frac{\langle \theta_H S_{xx} \rangle_\sigma - \langle \theta_H \rangle_\sigma \langle S_{xx} \rangle_\sigma}{\langle \theta_H \rangle_\sigma \langle S_{xx} \rangle_\sigma} = \frac{Q\rho}{S_{xx}R_H}, \quad (10)$$

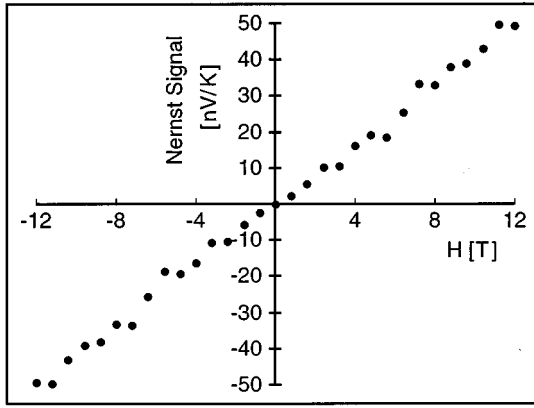


FIG. 2. Magnetic-field dependence of the raw Nernst signal at $T=250$ K showing the linear variation with the applied field strength.

which is experimentally obtainable as the ratio of four transport quantities—the Nernst coefficient Q , the resistivity ρ , the thermopower S_{xx} , and the Hall coefficient R_H . Note that $g^{S\theta_H}$ is the same as the ratio of the thermal Hall angle to the resistive hall angle, discussed in Ref. 7. Data for the dimensionless correlation $g^{S\theta_H}$ are shown in Fig. 4. Below $T = 280$ K, the correlation drops linearly, reaching zero at $T = 110$ K.

The variation around the Fermi surface of the Hall angle alone is available from a recent measurement of the normal-state magnetoresistance in $\text{YBa}_2\text{Cu}_3\text{O}_{7-\delta}$.² The dimensionless Hall-angle variance $\Delta\rho/[\langle\theta_H\rangle^2\rho]$ was observed to be independent of temperature in the oxygen-deficient 60-K phase of $\text{YBa}_2\text{Cu}_3\text{O}_{7-\delta}$, with a constant value of 1.7 between T_c and $T = 375$ K. In the fully oxygenated 90-K phase, the dimensionless variance changed slightly with temperature from 1.5 to 1.7 over the same range. The variation of the Hall angle around the Fermi surface in

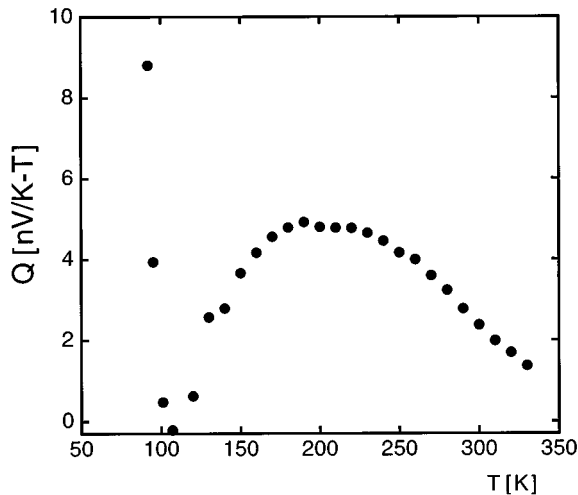


FIG. 3. Temperature dependence of the Nernst coefficient Q of the $\text{YBa}_2\text{Cu}_3\text{O}_{7-\delta}$ thin-film sample. Q goes to zero just above T_c , but increases rapidly at lower temperature, reflecting the large contribution from superconducting fluctuations.

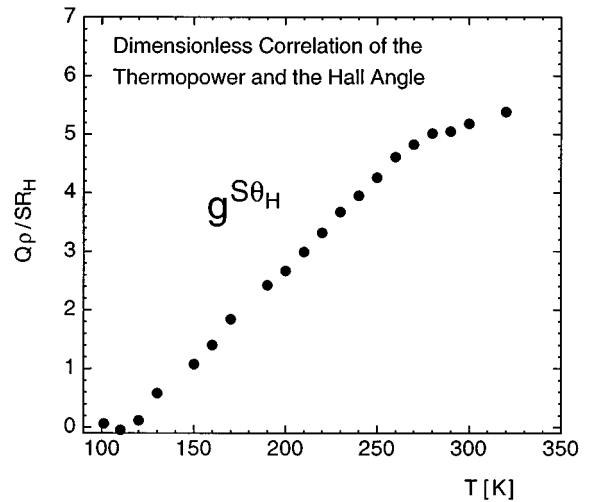


FIG. 4. Temperature dependence of the dimensionless correlation $g^{S\theta_H}$ between the Hall angle and the thermopower around the Fermi surface. The correlation goes to zero just above T_c in this sample of $\text{YBa}_2\text{Cu}_3\text{O}_{7-\delta}$.

$\text{YBa}_2\text{Cu}_3\text{O}_{7-\delta}$ is apparently related to a temperature-independent feature of the electronic structure of this compound.

The quantity $g^{S\theta_H}$, in contrast, is highly temperature dependent. The thermopower and the Hall angle lose all correlation in this sample just above T_c . A determination of whether or not this is a general feature in $\text{YBa}_2\text{Cu}_3\text{O}_{7-\delta}$ or is merely coincidental at this, nearly optimal, carrier concentration would require a systematic study at several different doping levels.

The orthorhombic crystal structure of $\text{YBa}_2\text{Cu}_3\text{O}_7$ permits two-dimensional Fermi surface variations of the transport quantities possessing both twofold and fourfold symmetry axes. The twofold variations can be measured directly as the a - b anisotropy of single crystal samples. The fourfold variations cannot be measured directly. In principle, however, once the a - b anisotropy has been characterized, the Nernst effect could be used to probe the fourfold variations of the thermopower. This approach would be most useful in tetragonal compounds such as $\text{Ti}_2\text{Ba}_2\text{Ca}_{N-1}\text{Cu}_N\text{O}_{4+2N}$, for which the magnetoresistance⁸ has been used to determine the fourfold anisotropy of the carrier relaxation time.

In summary, a simple formulation of the Nernst effect for anisotropic metals was introduced. Comparison was made with data from the normal state of the high- T_c superconductor $\text{YBa}_2\text{Cu}_3\text{O}_{7-\delta}$ and possible applications to the systematic study of the cuprates were discussed. In particular, the Nernst effect may be a useful probe of fourfold thermopower variations, distinguishing the $(0, \pi)$ and the (π, π) directions in k space.

I wish to thank C. W. Chu, Z. Y. Weng, C. S. Ting, D. M. Frenkel, and Y. Y. Xue for useful discussions. I thank Y. Y. Xue for a critical review of the manuscript. This work was supported in part by USAFOSR F49620-93-1-0310, NSF Grant No. DMR 91-22043, ARPA Grant No. MDA 972-90-J-1001, the Texas Center for Superconductivity at the University of Houston, and the T.L.L. Temple Foundation.

- ¹E. H. Sondheimer, Proc. R. Soc. London **193**, 484 (1948).
- ²J. M. Harris, Y. F. Yan, P. Matl, N. P. Ong, P. W. Anderson, T. Kimura, and K. Kitazawa, Phys. Rev. Lett. **75**, 1391 (1995).
- ³J. A. Clayhold, A. W. Linnen, Jr., F. Chen, and C. W. Chu, Phys. Rev. B **50**, 4252 (1994).
- ⁴Conductus, 969 W. Maude Avenue, Sunnyvale, CA 94086.
- ⁵A method of maintaining the isothermal boundary condition and eliminating contact misalignment in *malleable* materials is to bend the voltage contacts together, separated only by a thin, electrically insulating Kapton film, as in R. Fletcher, Philos. Mag. **25**, 87 (1972).
- ⁶R. P. Huebener, Physica B **97**, 588 (1994).
- ⁷Wu Jiang, S. N. Mao, X. X. Xi, Xiuguang Jiang, J. L. Peng, T. Venkatesan, C. J. Lobb, and R. L. Greene, Phys. Rev. Lett. **73**, 1291 (1994).
- ⁸N. E. Hussey, J. R. Cooper, J. M. Wheatley, I. R. Fisher, A. Carrington, A. P. Mackenzie, C. T. Lin, and O. Milat, Phys. Rev. Lett. **76**, 122 (1996).